Langmuir

ARTICLE

pubs.acs.org/Langmuir

Specific Ion Effects on Adsorption at the Solid/Electrolyte Interface: A Probe into the Concentration Limit

Jayanta M. Borah,[†] Sekh Mahiuddin,[*,†] Namrata Sarma,[†] Drew F. Parsons,[*,‡] and Barry W. Ninham[*,‡]

[†]Materials Science Division, North-East Institute of Science & Technology, CSIR, Jorhat-785 006, Assam, India

[‡]Research School of Physical Sciences and Engineering, Australian National University, Canberra 0200, Australia

ABSTRACT: Adsorption of organic acid at the mineral oxide−electrolyte interface has been explored. The adsorption of 2,4-dihydroxybenzoic acid onto α-alumina illustrates that specific ion effects show up at very low salt concentration (<0.05 mM). These surprising Hofmeister effects occur at salt concentrations an order of magnitude lower than in a previous study (*J. Colloid Interface Sci.* **2010**, *344*, 482). Salts enhance adsorption and specifically at ≤0.05 mM. With increasing concentration of ion, the adsorption density decreases. The results are accounted for by incorporating the ion size and dispersion forces in the theoretical modeling based on ab initio calculations of polarizabilities. The order appears to be governed by ion size, determining the maximum concentration that ions can attain near the surface due to close packing.

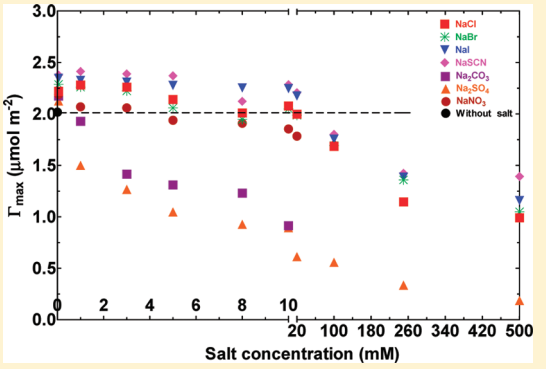

INTRODUCTION

Specific ion or Hofmeister effects are familiar mnemonics. They remind us that the classical theories of electrolyte solutions, interfaces, and colloidal interactions do not account for the behavior of real electrolytes. Systematic specificity of anion and cation and of ion-pair effects occur in a host of phenomena, in biological, colloidal, and geological systems. They are observed for example, in the different magnitudes of effects at interfaces (solid/liquid and liquid/vapor)[1−13] and at bulk physicochemical properties, e.g., surface tension, pH of buffer solutions, viscosity, activity coefficient, and freezing point depression.[14−20] Two recent books[21,22] describe various specific ion effects and the gradual progress toward theoretical understanding.[23]

The usual sequence that measures the relative efficiencies of salts on colloidal phenomena as a function of concentration is called a direct Hofmeister series. But sometimes the sequence is reversed in order.[6,24−28] Recent extensive literature traces ion specificity to the absence in classical theory of ion−ion and ion−substrate quantum fluctuation (dispersion) forces.[22] The inclusion of both ionic dispersion forces and of surface hydration effects, themselves in part due to these nonelectrostatic potentials, seems necessary and sufficient to explain direct and reverse ion specificity.[4,6,29−33]

The present work on reversed Hofmeister series at extremely low and high salt concentration provides a challenge to theory.

The solid (mineral)−water interface is of more than academic interest due to its ubiquity in plant biology and in the minerals industry.[34−39] In the millimolar salt concentration region, limited information exists on specific ion effects.[12,13,40,41] Most work focuses on ion specificity at the oxide−water interface that occurs at >0.1 M.[5,42,43]

Recently, we have demonstrated that even at concentrations as low as 0.5 mM both mono- and divalent ions markedly affect the adsorption of organic acids at the aluminum oxide/water interface.[12,44] In contrast, the occurrence of the specific ion effects in many system has been reported at higher salt concentration that roughly coincides with biological concentrations.[45]

The mineral−water interface is a singularly important interfacial system.[34−38] This is because many chemical processes in the aquatic ecosystem occur on mineral surfaces in the presence of organic acids (root exudates and released by microbes) and inorganic ions. There has been limited work on the quantification of the lowest possible salt concentrations, inevitably surface dependent also, at which the specific ion effects occur, either in bulk or for interfacial properties.

With that in mind, we have examined the influence of inorganic anions on the adsorption of dihydroxybenzoic acid (DHBA) onto aluminum oxide surface. It is of particular interest to us to quantify the minimum and maximum concentration of a salt required for appearance of the specific ion effects.

We report the adsorption of 2,4-dihydroxybenzoic acid (2,4-DHBA) onto alumina surfaces in aqueous medium as a function of concentration of different ions. We shall also give theoretical justification for the experimental results.

Parenthetically we remark on the reason for selection of 2,4-DHBA among all the available DHBAs. The electron-resonating effect and the inductive effect of the phenolic −OH group at ortho and para positions produce maximum electron density in the benzene ring and probably in the −COOH group. This results in a higher adsorption density in comparison to, e.g., 2-hydroxybenzoic and 4-hydroxybenzoic acids onto the alumina

Received: February 17, 2011
Revised: May 30, 2011
Published: June 14, 2011

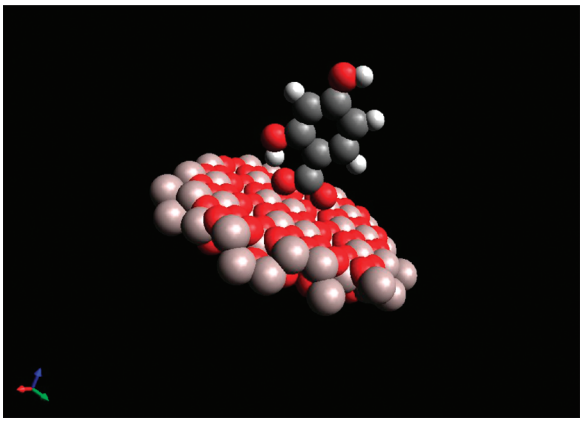

Figure 1. Illustration of alumina and 2,4-DHBA interaction. Color coding: Al (brown), O (red), C (black), and H (white).

surface.[46] The interaction that we have envisaged, of 2,4-DHBA with the alumina surface, on the basis of the preliminary ab initio simulation, is illustrated in Figure 1, and the detailed interaction of all isomers of DHBAs will be reported separately.

MATERIALS AND METHODS

Materials. α-Alumina (>99.7%, Aldrich) was washed twice with double-distilled water to remove any soluble impurities, dried, and finally heated at ∼700 °C for 3 h to remove gases and surface moisture and kept under vacuum. 2,4-DHBA (97%, Alfa Aesar), sodium hydroxide (>99%, s.d. fine-chem), and hydrochloric acid (AR grade, NICE Chemicals) were used without further purification. The salts used, NaCl (99.5%, Merck), NaBr (99.5%, Merck), NaI (99.5%, BDH), $NaNO_3$ (99.5%, Merck), NaSCN (99%, Loba Chemie), and Na_2SO_4 (AR, Rankem), were recrystallized from double-distilled water, dried, and kept in a vacuum desiccator, and Na_2CO_3 (99.5%, Nice Chemicals) was used as received. All solutions were prepared using freshly prepared double-distilled water.

Adsorption Isotherms. The experimental adsorption isotherms of 2,4-DHBA onto α-alumina surface were measured at pH 5 and 25 °C in a screw-capped glass tube. A suspension of 15 mL containing 0.5 g of α-alumina in the presence of either NaCl(aq), NaBr(aq), NaI(aq), $NaNO_3$-(aq), NaSCN(aq), Na_2CO_3(aq), or Na_2SO_4(aq) was mixed thoroughly with the help of a vortex mixer. The concentration of each salt was varied from 0.05 to 500 mM. The pH of the suspension was adjusted to 5 ± 0.1 using dilute HCl solution and then the suspension was allowed to equilibrate for 1 h in a refrigerated shaking water bath (SX-10R, Titec) maintained at 25 ± 0.1 °C. The required amount of 2,4-DHBA was added and the pH of the suspension was readjusted, if necessary. The suspension was further allowed to equilibrate for 60 min (duration of equilibrium adsorption). After equilibration, ∼10 mL of the suspension was filtered through a membrane of 0.2 μm pore size. Organic acids with −COOH and −OH groups are surface-active but not like a typical surfactant. These acids have a propensity for affinity with surfaces and are likely to adsorb on the filtering medium. So to avoid uncertainty in the concentration in the filtrate a few milliliters were rejected and the rest was collected for analysis. The residual concentration of 2,4-DHBA was estimated at the absorption maxima, λ_{max}, of 291.8 nm with a UV−visible spectrophotometer (SPECORD 200, Analytikjena). The adsorption density, Γ, of 2,4-DHBA was estimated from the mass balance equation

$$\Gamma = \frac{(C_0 - C_e)V}{ma} \quad (1)$$

where C_0 and C_e are the initial and residual concentration in millimolar of 2,4-DHBA in the suspension, V is the total volume of the suspension taken, and m and a are the mass and surface area of α-alumina, respectively.

Specific Ion Effects on pH. To understand further the specific ion effects on the pH that were demonstrated recently,[25,28] the pH of a series of 0.25 mM 2,4-DHBA solutions as a function of salt (NaCl, NaBr, NaI, $NaNO_3$, NaSCN, Na_2SO_4, Na_2CO_3) concentration (0.05−600 mM) was measured with a pH meter (Model 335, Systronics) and a combined glass electrode at 25 °C. The pH meter was calibrated at two points (pH 4 and 7) using standard buffer solutions prepared from buffer tablets (Qualigens Fine Chemicals). The uncertainty of the pH was ±0.10.

Theoretical Methods. In theoretical calculations, we estimate the adsorption density of 2,4-DHBA via the surface excess, Γ_{DHBA},[47,48]

$$\Gamma_{DHBA} = \int_0^\infty dz[c_{DHBA}(z) - c_0] \quad (2)$$

c_0 is the bulk concentration of 2,4-DHBA, $c_{DHBA}(z)$ is the concentration of 2,4-DHBA at a distance z from the surface. The surface excess describes the amount of ion adsorbed to a surface by physisorption (through electrostatic and dispersion interactions). It is calculated as the difference in ion concentrations near the surface (integrated over the whole surface region) from the bulk concentration of the ion. The experimental method measures the specific surface adsorption of 2,4-DHBA via the ion-specific spectroscopic measurement of residual 2,4-DHBA concentration using eq 1. Theoretical calculations are therefore likewise given for the specific surface excess Γ_{DHBA} of 2,4-DHBA, rather than the total surface excess, $\Gamma = \Sigma_i\Gamma_i$, summed over all ions. The total surface excess would correspond to the adsorption density measured, for instance, by QCM balance techniques, which are not specific to a single ion. Note that trends in the total surface excess are predicted to be similar in ion specificity to those reported here for the DHBA surface excess.

The 2,4-DHBA concentration profile, $c_{DHBA}(z)$, is calculated using a Poisson−Boltzmann model including ion−surface dispersion interactions. The theory used to analyze the data is highly technical and developed in a number of previous papers.[4,6,29−33] Here we give only a brief outline. Ion concentration profiles at the model alumina surfaces were calculated using the nonlinear Poisson−Boltzmann model with constant surface charge. Under the Poisson−Boltzmann model, the Poisson equation for the electrostatic potential, ψ, is solved self-consistently with an electrolytic charge distribution given by $\rho(z) = \Sigma_i q_i c_i(z)$, where the ion concentration profiles, $c_i(z)$, are established by the Boltzmann relation, $c_i(z) = c_{i0}\exp[-(q_i\psi(z) + U_i^{disp}(z))/kT]$. c_{i0} is the bulk concentration of ion i, and q_i is its charge. Three ions were used in the Poisson−Boltzmann calculation, the two anions 2,4-DHBA and the salt anion; the third ion, Na^+, was their counterion. The bulk concentration, c_0, for the 2,4-DHBA anion was fixed at 1 mM, while the bulk concentration c_{salt} of added salt was varied from 0 to 500 mM. The specific concentration of ions was set by using the following procedure, designed to match the experimental procedure, by varying the relative concentrations as total added salt is varied. For simplicity, hydrogen ions were not explicitly included, since at pH 5 their concentration (0.01 mM) relative to other ions is negligible. c_0[DHBA] was fixed at 1 mM (assumed to be completely deprotonated into anionic form). The inorganic anion concentration was given by salt concentration, c_0[anion] = c_{salt}. The Na^+ concentration was set in a manner mimicking the experimental procedure. The natural pH of 2,4-DHBA at mM concentrations falls below 3. The experimental procedure adds NaOH to restore the pH back to 5. We model this step in theoretical calculations by setting $c_0[Na^+] = c_{salt} + c_0$[DHBA] (a more sophisticated model including explicit H^+ would also subtract $c_0[H^+]$ here). Ion concentrations, $c_i(z)$, were constrained with a cap preventing them from surpassing close-packed concentrations, given by $1/V_i$, where V_i (=$4\pi d_i^3/3$) is the ionic volume due to a hard sphere ion of radius d_i. One deficiency of the Poisson−Boltzmann model is that it neglects ion−ion correlations and certain finite size effects [which are included in higher level integral

dx.doi.org/10.1021/la2006277 |Langmuir 2011, 27, 8710–8717

Table 1. Ion Parameters Used in Theoretical Calculations[a]

ion	α_0 (Å^3)	a_i (Å)	d_i (Å)	B (10^{-50} J m^3)	$U_i^{disp}(z=0)$ (kJ/mol)
$Na^+ \cdot 3H_2O$	4.14	2.250	2.474	−0.4929	−0.784
$SO_4^{2-} \cdot 3H_2O$	12.63	3.332	3.664	2.7385	1.341
$CO_3^{2-} \cdot 4H_2O$	15.56	3.171	3.486	−1.3840	−0.787
NO_3^-	5.02	2.012	2.213	−2.6176	−5.821
Cl^-	4.86	1.861	2.046	−2.0225	−5.690
Br^-	6.49	1.968	2.164	−2.7851	−6.620
I^-	9.65	2.121	2.332	−4.1100	−7.802
SCN^-	8.13	2.178	2.394	−3.9442	−6.921
2,4-DHBA	16.20	2.815	3.095	−9.3768	−7.619

[a] a_i is the Gaussian radius used in ion dispersion interactions, d_i is the hard sphere radius, B is the ion−surface dispersion coefficient. $U_i^{disp}(z=0)$ is the ion−surface dispersion interaction evaluated at contact with the surface. The static polarizability α_0 (ab initio calculation in vacuum) is also given for reference.

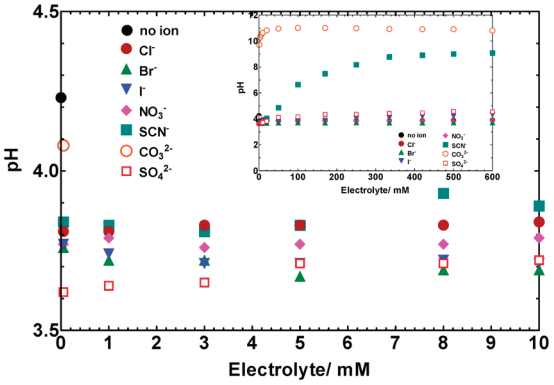

Figure 2. pH of 0.25 mM 2,4-DHBA solutions (filled black circle) and in the presence of different salts as a function of concentration (0.05−10 mM). The inset shows the pH variation in the presence of the same salts at 0.05−600 mM.

equation methods such as hypernetted chain (HNC)].[49] Capped concentrations partially alleviate this deficiency and are crucial to reproduce in theory the experimental order of ions, as discussed later. Furthermore, if they are not introduced, then uncapped concentrations may suppress calculated surface excesses of 2,4-DHBA by an order of magnitude (e.g., from 1 μmol/m^2 at 200 mM salt concentrations, consistent with experiment, down to 0.1 μmol/m^2).

The parameter U_i^{disp} is an ion−surface dispersion interaction given by

$$U_i^{disp}(z) = f_i(z)B/z^3 \quad (3)$$

where $f_i(z) = 1 + (2z/\pi^{1/2}a_i)[2z^2/a_i^2 - 1]\exp(-z^2/a_i^2) - [1 + 4z^4/a_i^4]\,\mathrm{erfc}(z/a_i)$, keeping the interaction energy finite at $z = 0$, where $U_i^{disp}(z=0) = 16B/(3\pi^{1/2}a_i^3)$. This expression incorporates the finite size of the ion, with parameter a_i corresponding to the Gaussian radius of an ion with Gaussian spatial spread.[30] The hard sphere ion of radius d_i is related to a_i.[30] The value of the ion−surface dispersion coefficient, B, is derived from the dynamic polarizability $\alpha_i(i\omega)$ of the ion and accounts for the surrounding aqueous medium.[29] The kosmotropic ions Na^+, SO_4^{2-}, and CO_3^{2-} are taken to have strongly held hydration shells,[6,31] with hydration numbers of 3, 3, and 4, respectively, following Marcus.[50] The simple shell model of Parsons and Ninham[31] is applied to SO_4^{2-} and CO_3^{2-}. In the case of Na^+, however, explicit hydration is used, with ab initio dynamic polarizabilities calculated for the whole $Na^+ \cdot 3H_2O$ cluster.

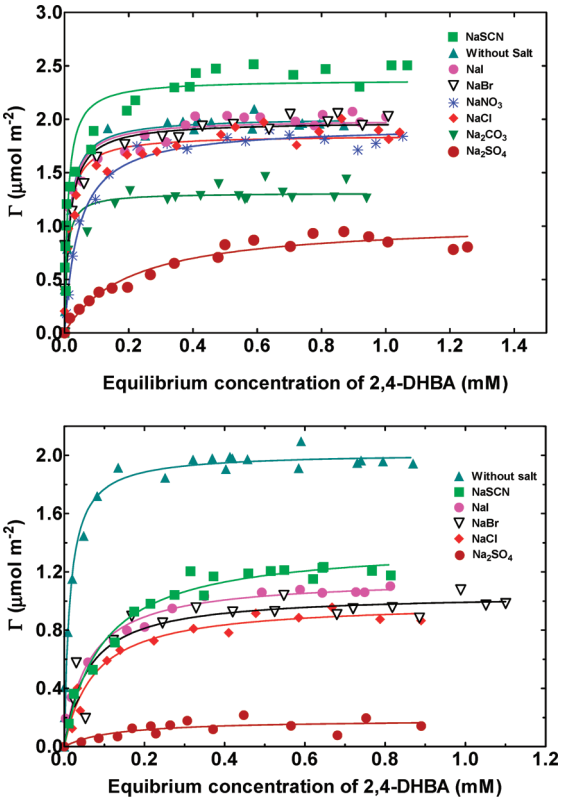

Figure 3. Adsorption isotherms of 2,4-DHBA onto α-alumina in the presence of different anions, with sodium as the common cation, at pH 5 and 25 °C: (a) 5 mM salt and (b) 500 mM salt. The symbols represent the triplicate experimental data, and the lines are the theoretical values calculated from the Langmuir equation, $\Gamma = (\Gamma_{max}C_e)/(K + C_e)$, where C_e is the equilibrium concentration of an acid, $K = 1/K_s$ (K_s is the adsorption coefficient), and Γ and Γ_{max} are the adsorption densities of an acid in μmol m^{-2} at equilibrium and after saturation of α-alumina surfaces, respectively.

Five-mode parametrizations of the ab initio dynamics polarizabilities of polyatomic ions and hydrated $Na^+ \cdot 3H_2O$ are given in the Appendix. Parametrizations for the halides have been published elsewhere.[29]

The alumina surface charge was taken to be 0.81 C m^{-2}, fitted to reproduce the experimental 2,4-DHBA surface excess of 2 μmol/m^2 from 1 mM DHBA in 10 mM NaCl. This surface charge is of the same order of magnitude but higher than that (0.4 C m^{-2}) expected from alumina charge regulation models.[51] The position of "infinity" (the cutoff position far from the surface) is taken as 10 times the Debye length of the solution, allowing the electrostatic field to fall to zero.

The ion size parameters and dispersion B coefficients (against alumina) are presented in Table 1 along with the value of the ion−surface dispersion energy calculated at contact with the surface.[30]

RESULTS AND DISCUSSION

Ion Effects on the pH of 2,4-DHBA. A typical plot of pH of 0.25 mM 2,4-DHBA solution vs concentration of different sodium salts up to 10 mM is shown in Figure 2 and in a wide concentration range typically up to 600 mM in Figure 2 (inset). It is interesting to note that 2,4-DHBA at 0.25 mM has pH 4.23 and upon addition of different salt below 50 mM there is typically a decrease of ≥0.15 pH units (Figure 2). In contrast, the pH of 0.25 mM 2,4-DHBA solution increases sharply as a function of Na_2CO_3 concentration up to 50 mM, and above this concentration the pH remains

dx.doi.org/10.1021/la2006277 |Langmuir 2011, 27, 8710–8717

constant (Figure 2, inset). Unlike the clear direct and reverse specific ion effects in pure water and buffer solutions,[28] no remarkable salt-induced change in pH value was observed except for SCN^- at ≥50 mM and CO_3^{2-} at ≥1 mM; see Figure 2 (inset). Further, the kosmotropes and the chaotropes within the concentration range (up to 600 mM) do not exhibit any clear Hofmeister series sequence. We remark here that the cause of the typical impact of anions on the pH of 0.25 mM 2,4-DHBA solution may be due to the change in intra- and intermolecular associations of 2,4-DHBA. This subject is beyond the scope of the present study and to be explored separately.

Adsorption Isotherms at Different Concentrations of Salts. The adsorption isotherms of 2,4-DHBA onto α-alumina surfaces at different concentrations (0.05−500 mM) of NaCl(aq), NaBr(aq), NaI(aq), $NaNO_3$(aq), NaSCN(aq), Na_2CO_3(aq), and Na_2SO_4(aq), pH 5 and at 25 °C were carried out. Two typical examples of the adsorption isotherms in the presence of 5 and 500 mM of different anions are shown in Figure 3a,b. It is apparent from the plot that there exist significant specific ion effects at both 5 and 500 mM salt concentrations. The order of specific ion effects on the experimental Γ_{max} (maximum adsorption density; see the caption of Figure 3), taking Cl^- as the reference in the Hofmeister anion series, follows $SO_4^{2-} < CO_3^{2-} < NO_3^- < Cl^- \approx Br^- < I^- < SCN^-$ (Figure 3a) and $SO_4^{2-} < Cl^- < Br^- < I^- < SCN^-$ (Figure 3b). At 500 mM in the presence of CO_3^{2-} and NO_3^-, no significant adsorption of 2,4-DHBA was observed.

A possible reason is that CO_3^{2-} and NO_3^- compete with 2,4-DHBA for the surface sites and preferentially adsorb onto α-alumina, covering much of the available surface. Further note that at higher salt concentration (comparison of Figure 3, parts a and b) the magnitude of the adsorption density of 2,4-DHBA onto α-alumina in the presence of a particular ion is much lower, which indicates a comparatively higher degree of adsorption of CO_3^{2-} and NO_3^- over 2,4-DHBA. This presumably is linked with the higher surface propensity of CO_3^{2-} and NO_3^-. CO_3^{2-} and NO_3^- are known to adsorbed at the oxide−water interface,[52−55] and note that CO_3^{2-}, as a cosolute, greatly influences the adsorption of anions onto the mineral surface. A similar situation holds in the present system.

In a previous paper[12] we showed that the sequence in adsorption densities at surface saturation, Γ_{max}, of *p*-hydroxybenzoate on the α-alumina surfaces in the presence of different anions at 0.5 mM representing the specific ion effect is $S_2O_3^{2-} < SO_4^{2-} < Cl^- > Br^- > I^- > NO_3^-$. Taking Γ_{max} as the parameter to examine the specific ion effects, it is interesting to note that at 5 and 500 mM salt concentration the sequence follows $SO_4^{2-} < CO_3^{2-} < Cl^- \sim NO_3^- < Br^- < I^- < SCN^-$; at 500 mM, CO_3^{2-} and NO_3^- are absent. The specific ion effects particularly for the halides in 2,4-DHBA/α-alumina and *p*-hydroxybenzoate/α-alumina systems are the opposite in nature. Hofmeister reversal or reordering is not a new observation. Nonetheless, it is surprising and of relevance to oxide/water systems. Contrary to direct or reverse specific ion effects at the solid/water interface,[6,56−62] we observed both reverse specific ion effects for the chaotropes and direct specific ion effects for the kosmotropes in the same system. The occurrence of such direct and reverse specific ion effects can be accounted for by incorporation of hydration forces associated with the nonelectrostatic potentials.[6] It has been modeled by using both nonpolarizable and polarizable force fields.[63] But the apparent success of such models for the adsorption of ions depends on the relative competition of an ion and the surface in the structuring of neighboring water and their interplay with the

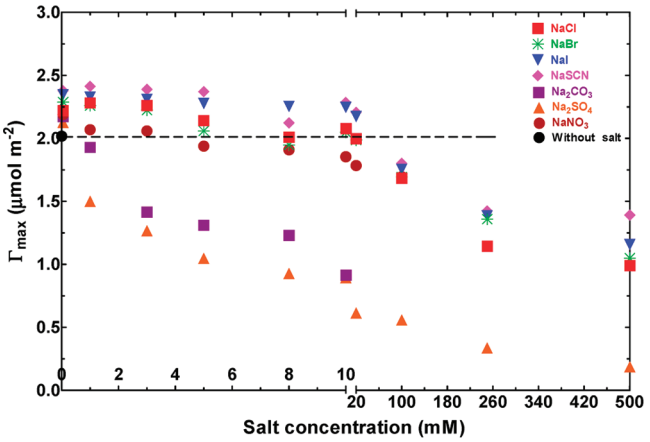

Figure 4. Plots of Γ_{max} (defined in Figure 2 caption) vs electrolyte concentration for adsorption of 2,4-DHBA onto α-alumina at pH 5 and 25 °C.

isoelectric point (IEP) of the surface.[5,64−66] Thus, Hidber et al.[67] demonstrated that the adsorption of an adsorbate (phenolic compounds and organic acids) onto the alumina surface causes a lowering of the IEP. Further, a low IEP surface (e.g., silica) is a structure-breaking surface while a surface with high IEP is a structure-making surface.[5] Note that ionic polarizability is a key determinant of the ion specificity sequence.[23,68,69] The existence of a direct or reverse Hofmeister sequence among the ions depends on both the system and the concentration of ions and plays in a complex manner.[5,68,70−76]

The results of molecular dynamics simulations of halides at the water/vapor interface[10,77−79] inferred that the higher the polarizability, the higher the propensity for the interface. So, according to the polarizability of the ion [SO_4^{2-} (6.33 Å^3), CO_3^{2-} (5.06 Å^3), NO_3^- (4.48 Å^3), Cl^- (3.76 Å^3), Br^- (5.07 Å^3), I^- (7.41 Å^3), SCN^- (6.74 Å^3)][80] I^-, SO_4^{2-}, and SCN^- have a higher surface propensity and the adsorption density of 2,4-DHBA should be lower in the presence of these higher polarizable ions. In fact, only the polarizability factor of SO_4^{2-} is in tune with the experimental results (Figure 3a,b). So, we comment here that the polarizability factor of ions alone is not the governing factor for lowering of the adsorption density and the specific ion effects. The ion specificity sequence on the experimental Γ_{max} for the halides at 5 and 500 mM, according to polarizability, should have been $Cl^- > Br^- > I^-$, i.e., reverse of the polarizability sequence, but the experimental results follow the polarizability sequence (Figures 3a,b).

Therefore, the kosmotropes have the "correct" sequence while the chaotropes exhibit a reverse specific ion effect for the present system. The possible reason for the reverse specific ion effects of chaotropes may be accounted for by (i) the change of the IEP of α-alumina upon adsorption of adsorbate,[67] (ii) that 2,4-DHBA competes over inorganic chaotropes for the surface sites, and (iii) the different hydration forces of ions[6] in the presence of 2,4-DHBA. In the light of the theoretical analysis given below, the second possibility seems most likely, taken with a steric effect due to the finite size of the ions, which gives a maximal capped concentration of ions in the surface region.

Concentration Dependence of the Specific Ion Effect. The variation of adsorption density at surface saturation, Γ_{max}, as a function of salt concentration is shown in Figure 4. It is interesting to note that ions at very dilute concentration (≤0.05 mM) markedly enhance the adsorption of 2,4-DHBA

dx.doi.org/10.1021/la2006277 |*Langmuir* 2011, 27, 8710–8717

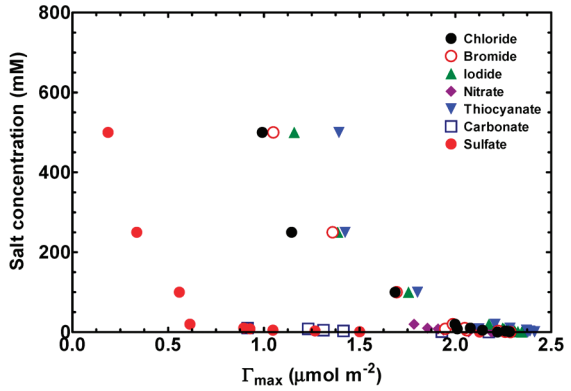

Figure 5. Salt concentration vs adsorption maxima of 2,4-DHBA of different electrolyte at pH 5 and 298.15 K.

onto α-alumina. The promotive effect gradually decreases with the increase in concentration of ions, as is evident from the decrease in adsorption density of 2,4-DHBA. We further infer from Figure 4 that at a certain concentration ions inhibit adsorption of 2,4-DHBA. We take this up in the subsequent discussion of Figure 5. There are evidently quite different specific ion effects at low and high salt concentrations. Limited work has been done on specific ion effects over a wide range concentration of different salts.[12,13,27,68,81,82] The specific ion effect in the cloud-point temperature of lysozyme exhibits a direct sequence at high salt concentration (>300 mM) and inverse at lower concentrations (<300 mM) at pH 9.4.[68] Note that the anion effect for the restriction enzymatic activities in two buffer systems is significantly different than that of direct or reverse Hofmeister series.[27] The direct and reverse specific ion effects are also system specific.[27,28] This is not a surprise if it is recognized that ion−surface dispersion forces are involved.[27] Further, direct and reverse specific ion effects have been observed in the inhibition of protein precipitation at lower salt concentration (0.005 M) and salt-induced precipitation at higher concentration (4 M).[83] For the solid−liquid interface, practically all the literature on specific ion effects focuses on high electrolyte concentrations, typically >0.1 M,[5,42,43] and only in a few cases at lower concentrations than this.[12,40,41] The question remains, what is the minimum and maximum concentrations of salt required to generate specific ion effects in physicochemical properties of a system?

Concentration Limit for the Specific Ion Effects. Note that the adsorption density at surface saturation, Γ_{max}, at 0.05 mM salt concentration increases as compared with that without salt (Figure 4). At this salt concentration, the sequence of the specific ion effects follows SO_4^{2-} (Γ_{max} = 2.13) < CO_3^{2-} (Γ_{max} = 2.17) < NO_3^- (Γ_{max} = 2.19) < Cl^- (Γ_{max} = 2.22) < Br^- (Γ_{max} = 2.29) < I^- (Γ_{max} = 2.35) < SCN^- (Γ_{max} = 2.38). The difference in the magnitudes of Γ_{max} is not remarkable but is in line with the sequence for 5 mM salt concentration. Taking the Γ_{max} without salt as the reference, the kosmotropes (CO_3^{2-} and SO_4^{2-}) exhibit a significant influence in Γ_{max} at much lower concentration (1 mM, negative departure from the dotted baseline) as compared with all other ions at 100 mM.

The present experimental results indicate that the specific ion effects can be observed at 0.05 mM or even at much lower concentration. These experimental findings contradict the claims of Lyklema.[84] The concentration of salts has a significant influence on the specific ion effect; e.g., at lower concentration it is reverse Hofmeister series in the cloud-point temperature of lysozyme, and at higher concentration it is direct.[68] In the present system, the specific ion effects are reversed for the chaotropes with some noticeable exceptional behavior of NO_3^-, which we now discuss. At low concentration (≤5 mM) it is noted that NO_3^- behaves like a kosmotope but at higher concentration, say at 100 mM, it is a chaotrope [SO_4^{2-} (Γ_{max} = 0.56) < Cl^- (Γ_{max} = 1.69) ∼ Br^- (Γ_{max} = 1.69) ∼ NO_3^- (Γ_{max} = 1.70) < I^- (Γ_{max} = 1.76) < SCN^- (Γ_{max} = 1.80), Figure 4]. Earlier, we observed that NO_3^- does not exhibit a specific ion effects that would be expected from its polarizability alone. So, the theoretical origin for the specific ion effect of NO_3^- is likely to be different.

Table 2. Maximum Electrolyte Concentration for Zero Adsorption Density of 2,4-DHBA onto α-Alumina Surface at pH 5 and 298.15 K

background electrolyte	maximum electrolyte concentration (mM)
NaSCN	∼1412
NaCl	∼918
NaBr	∼1129
NaI	∼1207
Na_2SO_4	∼659
$NaNO_3$	∼125
Na_2CO_3	∼23

Rather, the specific ion effects sequence that appears in our studies is due to the competing ion specific properties of polarizability, anisotropy, and ion size. Ionic dispersion forces, especially close to the surface, are strengthened as polarizability increases but generally weakened as ion size increases. This rule may be illustrated by considering the ion−surface dispersion interaction energy, eq 3, at contact (z = 0). The contact dispersion energy is $U_i^{disp}(z=0) = 16B/3\pi^{1/2}a_i^3$). When the ion polarizability is larger, the dispersion coefficient B is larger (see Appendix). But when the ion size is larger, expressed here through radius a_i, the strength of the dispersion interaction close to the surface is diminished inversely proportionally to the ion volume (that is, the cube of the radius). (Ion size can also have an indirect effect, diminishing the magnitude of the dispersion B coefficient, by reducing the magnitude of the excess polarizability, which is the effective polarizability of the ion inside a cavity surrounded by the solvent). For instance, the B coefficients of hydrated SO_4^{2-} and Br^- have almost identical magnitudes, nearly 2.7 × 10^{-50} J m^3, but the larger size of the hydrated SO_4^{2-} ion results in a significantly lower magnitude of the dispersion energy at contact, as seen in Table 1.

The adsorption density at surface saturation, Γ_{max}, of an adsorbate, here 2,4-DHBA, onto an adsorbent decreases with the increase in concentration of a salt (Figure 4). So, we presume that at certain concentration of a salt, there would be no adsorption of an adsorbate. To explore this proposition, a typical plot of salt concentration vs Γ_{max} of 2,4-DHBA onto an α-alumina surface at pH 5 and 298.15 K is shown in Figure 5.

Figures 4 and 5 are used to estimate the possible maximum salt concentration at which the adsorption density of 2,4-DHBA approaches zero. The maximum salt concentration is different for different salts. Table 2 shows the maximum theoretical concentration of different salts for zero adsorption density of 2,4-DHBA onto α-alumina surface at pH 5 and 298.15 K. The reasons for no adsorption of 2,4-DHBA at higher salt concentration are likely to be 2-fold: First, from a classical point of view, the thickness of the

dx.doi.org/10.1021/la2006277 |*Langmuir* 2011, 27, 8710–8717

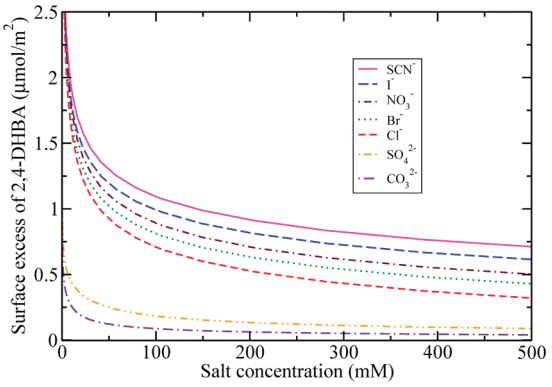

Figure 6. Surface excess of 2,4-DHBA, initial concentration 1 mM, as a function of salt concentration. Ion concentrations are capped according to specific ion volumes.

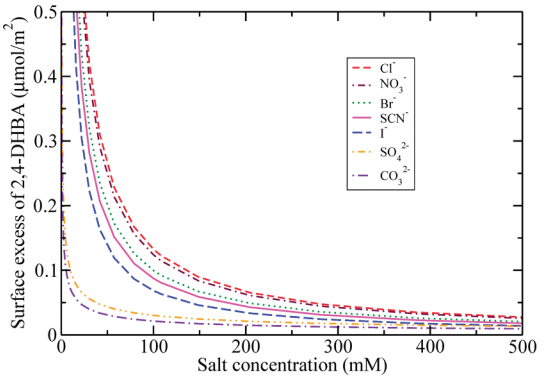

Figure 7. Surface excess of 2,4-DHBA, initial concentration 1 mM, as a function of salt concentration. Ion concentrations are uncapped.

double layer decreases and the closest approach of ions becomes minimum. Anions, according to the magnitude of polarizability, exhibit more surface propensity in comparison to 2,4-DHBA and anions preferentially cover the surface site of alumina. Second, with the increase in salt concentration, the surface hydration and the electrostatic and dispersion forces increase, resulting in zero adsorption density of 2,4-DHBA at respective critical salt concentrations. The latter approach is the backbone of our theoretical calculation.

Note that in the presence of NO_3^- and CO_3^{2-} at 100 and 23 mM, respectively, 2,4-DHBA does not adsorb (Figure 4) onto an α-alumina surface. The unusual adsorption behavior of NO_3^- is due to its geometrical structure. The nonspherical, flat structure and the three oxygen atoms in the nitrate ion result in different hydration and adsorption geometries that cause NO_3^- to compete against 2,4-DHBA and occupy the entire available surface site. A similar explaination may also be drawn for CO_3^{2-}. Therefore, at higher salt concentration both kosmotropes and chaotropes compete against 2,4-DHBA and are preferentially adsorbed onto α-alumina surface and cover all the surface sites.

Theoretical Results. Theoretical calculations of the surface excess of 1 mM 2,4-DHBA at the alumina surface are shown in Figure 6 as a function of the concentration of the various ions considered. The predicted series is $CO_3^{2-} < SO_4^{2-} < Cl^- < Br^- < NO_3^- < I^- < SCN^-$. This agrees somewhat with experiment (Figure 4), with CO_3^{2-} on the wrong side of SO_4^{2-} and NO_3^- misplaced. The magnitudes of adsorption densities also agree reasonably well with experiment (the surface charge was fitted to reproduce a surface excess of 2 μmol/m^2 in 10 mM NaCl).

The calculations shown in Figure 6 include ion concentrations capped by the volume of each ion (a simple method of constraining their concentrations to below close-packed levels). If this constraint is removed, allowing ion concentrations to exceed 100 M, for instance, then the surface excesses are obtained in the order $CO_3^{2-} < SO_4^{2-} < I^- < SCN^- < Br^- < NO_3^- < Cl^-$, as shown in Figure 7. That is, an *entirely* wrong order is obtained. This highlights the significance of ion size, in conjunction with ion dispersion interactions, in controlling the ion specificity.

The significance of the role of capped concentrations (that is, ion size) provides some insight into the anomaly with CO_3^{2-} and NO_3^-. Both of these ions are planar (as is 2,4-DHBA). It would seem that the simple inverted volume method used to enforce capped concentrations, which assumed a close packing of spherical ions, is too crude a model for these planar ions. The planar anisotropy will also affect the ion−surface dispersion interaction; a spherical Gaussian ion shape was assumed for the dispersion calculations applied here. Additionally, higher order multipole dispersion interactions[85] (induced quadrupoles and octupoles) are likely to play an important role for the polyatomic ions. These points should apply also to the linear ion SCN^-, but the relative success of the theoretical calculation of SCN^- suggests that anisotropies are less important for this linear ion than for planar ions.

The limitations of the Poisson−Boltzmann approach can be inferred from the low concentration behavior in Figure 6. Even though concentrations have been capped, the curves do not take a flat asymptote near 2 μmol/m^2, as seen in Figure 4. This is likely due to other finite size effects, such as ion−ion correlations, neglected in the Poisson−Boltzmann model but accessible to more sophisticated HNC modeling.[49]

CONCLUSIONS

The adsorption of 2,4-DHBA, a well-defined organic acid, onto α-alumina surface is highly ion specific from very low concentration to high concentration. The higher concentration is the signature of the ion for the specific ion effects. At very low concentration (in this study it is 0.05 mM, may be still lower) ions promote the adsorption of 2,4-DHBA and the promotional effect gradually decreases as the concentration of ions increases, exhibiting specific ion effects. The kosmotropes (CO_3^{2-} and SO_4^{2-}) exhibit a significantly larger effect relative to other ions at much lower concentration. Nevertheless, both kosmotropes and chaotropes at higher concentration compete against 2,4-DHBA and no adsorption of 2,4-DHBA takes place. Theoretical Poisson−Boltzmann calculations based on ab initio dynamic polarizabilities showed that polarizability of ions alone is not responsible for the specific ion effects for adsorption of organic acids onto α-alumina surface. Rather ion size and dispersion forces are equally responsible for such effects. In particular, the order is governed by ion size, determining the maximum concentration that ions can attain near the surface due to close packing. Unlike direct or reverse specific ion effects, mixed specific ion effects (direct effect for kosmotropes and reverse for the chaotropes) are observed in the present system and govern the adsorption behavior of 2,4-DHBA onto α-alumina/water interface.

Table 3. Static Polarizabilities, Weights, and Characteristic Frequencies for Five-Mode Decompositions of the Dynamic Polarizabilities of Ions (see eq 5)[a]

		mode 1		mode 2		mode 3		mode 4		mode 5	
ion	α_0 (Å^3)	f_1	ω_1 (au)	f_2	ω_{12}(au)	f_3	ω_3 (au)	f_4	ω_4 (au)	f_5	ω_5 (au)
2,4-DHBA	16.1964	0.2607	0.2160	0.3577	0.4301	0.3305	0.8291	0.0494	1.8592	0.0016	6.6599
SCN^-	8.1278	0.2083	0.1968	0.5549	0.3724	0.2146	0.7569	0.0202	1.9560	0.0020	9.3554
NO_3^-	5.0215	0.3418	0.2536	0.3863	0.5638	0.2270	1.0631	0.0429	2.4249	0.0018	9.3252
CO_3^{2-}	9.8536	0.1981	0.0815	0.3821	0.1886	0.3148	0.5236	0.0987	1.2930	0.0058	4.4900
SO_4^{2-}	8.3492	0.2097	0.1784	0.3737	0.3708	0.3587	0.7817	0.0542	1.9666	0.0035	7.9423
$Na^+ \cdot 3H_2O$	4.1396	0.1931	0.3515	0.5170	0.6310	0.2485	1.2067	0.0397	2.6838	0.0018	9.3256

[a] 1 au = 6.57968×10^{15} Hz.

APPENDIX

Dispersion B coefficients determine the strength of ion dispersion interactions

$$B = \frac{kT}{2}\sum{}'\frac{\alpha^*(i\omega_n)}{\varepsilon_w(i\omega_n)}\frac{\varepsilon_w(i\omega_n)-\varepsilon_s(i\omega_n)}{\varepsilon_w(i\omega_n)+\varepsilon_s(i\omega_n)} \quad (4)$$

where the prime with Σ' means the zero frequency $n = 0$ term is taken with factor 1/2. The summation is made over Matsubara frequencies $\omega_n = 2\pi kTn/\hbar$. The parameter ε_w is the dielectric function of water,[86] and ε_s is the dielectric function of the alumina surface.[87] The asterisk with α^* indicates that the ion polarizability is transformed from its value in vacuum to an effective (excess) polarizability in water.[29]

Dynamic polarizabilities of ions in vacuum were calculated by ab initio quantum chemical software. Electron correlation was provided through the coupled cluster singles and doubles (CCSD) level of theory for the monatomic ions[29] and via DFT with the PBE0 functional for polyatomic ions. The aug-cc-pV*Z family of basis sets was used. The ECP28MDF[88] effective core potential (pseudopotential) was used for the larger I^- ion. The geometry of polyatomic ions (and triply hydrated Na^+) was first optimized to minimize energy before calculating polarizabilities.

For convenience, the ab initio polarizabilities may be fitted to a multimode sum

$$\alpha(i\omega) = \alpha_0 \sum_j \frac{f_j}{1+(\omega/\omega_j)^2} \quad (5)$$

where α_0 is the static polarizability and $\Sigma_j f_j = 1$. The error in the fit over five modes is around 0.02%.[29] Fitted modal coefficients $\{f_j, \omega_j\}$ for the halides have been reported previously.[29] In Table 3 we give the parameters of a five-mode fit for 2,4-DHBA, along with SCN^-, NO_3^-, CO_3^{2-}, SO_4^{2-}, and $Na^+ \cdot 3H_2O$.

AUTHOR INFORMATION

Corresponding Author

*E-mail: mahirrljt@yahoo.com, mahiuddins@rrljorhat.res.in (S.M.), Drew.Parsons@anu.edu.au (D.F.P.), and barry.ninham@anu.edu.au (B.W.N.).

ACKNOWLEDGMENT

The authors (S.M., J.M.B., and N.S.) are grateful to the Department of Science and Technology, New Delhi, India, and Council of Scientific and Industrial Research, New Delhi, India, for the financial support. The authors are also thankful to the Director, North-East Institute of Science and Technology, CSIR, Jorhat, India, for the encouragement and facilities. We thank the anonymous reviewers for several valuable suggestions.

REFERENCES

(1) Cacace, M. G.; Landau, E. M.; Ramsden, J. J. *Q. Rev. Biophys.* **1997**, *30*, 241–277.
(2) Collins, K. D.; Washabaugh, M. W. *Q. Rev. Biophys.* **1985**, *18*, 323–422.
(3) Conway, B. E. *Electrochim. Acta* **1995**, *40*, 1501–1512.
(4) Salis, A.; Parsons, D. F.; Boström, M.; Medda, L.; Barse, B.; Ninham, B. W.; Monduzzi, M. *Langmuir* **2010**, *26*, 2484–2490.
(5) Franks, G. V.; Johnson, S. B.; Scales, P. J.; Boger, D. V.; Healy, T. W. *Langmuir* **1999**, *15*, 4411–4420.
(6) Parsons, D. F.; Boström, M.; Maceina, T. J.; Salis, A.; Ninham, B. W. *Langmuir* **2010**, *26*, 3323–3328.
(7) Yang, Z.; Li, Q.; Chou, K. C. *J. Phys. Chem. C* **2009**, *113*, 8201–8205.
(8) Chen, X.; Yang, T.; Kataoka, S.; Cremer, P. S. *J. Am. Chem. Soc.* **2007**, *129*, 12272–12279.
(9) Mucha, M.; Frigato, T.; Levering, L. M.; Allen, H. C.; Tobias, D. J.; Dang, L. X.; Jungwirth, P. *J. Phys. Chem. B* **2005**, *109*, 7617–7623.
(10) Jungwirth, P.; Tobias, D. J. *J. Phys. Chem. B* **2002**, *106*, 6361–6373.
(11) Jungwirth, P.; Tobias, D. J. *Chem. Rev.* **2006**, *106*, 1259–1281.
(12) Das, M. R.; Borah, J. M.; Kunz, W.; Ninham, B. W.; Mahiuddin, S. *J. Colloid Interface Sci.* **2010**, *344*, 482–491and references therein.
(13) Ao, Z.; Liu, G.; Zhang, G. *J. Phys. Chem. C* **2011**, *115*, 2284–2289.
(14) Zavitsas, A. A. *J. Phys. Chem. B* **2001**, *105*, 7805–7817.
(15) Hosoda, H.; Mori, H.; Sogoshi, N.; Nagasawa, A.; Nakabayashi, S. *J. Phys. Chem. A* **2004**, *108*, 1461–1464.
(16) Schleich, T.; Von Hippel, P. H. *Biopolymers* **1969**, *7*, 861–877.
(17) Boström, M.; Kunz, W.; Ninham, B. W. *Langmuir* **2005**, *21*, 2619–2623.
(18) Wachter, W.; Kunz, W.; Buchner, R. *J. Phys. Chem. B* **2005**, *109*, 8675–8683.
(19) Wahab, A.; Mahiuddin, S.; Hefter, G.; Kunz, W.; Minofar, B.; Jungwirth, P. *J. Phys. Chem. B* **2005**, *109*, 24108–24120.
(20) dos Santos, A. P.; Diehl, A.; Levin, Y. *Langmuir* **2010**, *26*, 10778–10783.
(21) Kunz, W., Ed. *Specific Ion Effects*; World Scientific: Singapore, 2010.
(22) Ninham, B. W.; Lo Nostro, P. *Molecular Forces and Self Assembly: In Colloid, Nano Sciences and Biology*; Cambridge University Press: Cambridge, 2010.
(23) Kunz, W.; Lo Nostro, P.; Nimham, B. W. *Curr. Opin. Colloid Interface Sci.* **2004**, *9*, 1–18.
(24) Pinna, M. C.; Salis, A.; Monduzzi, M.; Ninham, B. W. *J. Phys. Chem. B* **2005**, *109*, 5406–5408.

(25) Boström, M.; Loretti, B.; Fratini, E.; Baglioni, P.; Ninham, B. W. *J. Phys. Chem. B* **2006**, *110*, 7563–7566.
(26) Zhang, Y.; Cremer, P. S. *Curr. Opin. Chem. Biol.* **2006**, *10*, 658–663.
(27) Kim, H. K.; Tuite, E.; Norden, B.; Ninham, B. W. *Eur. Phys. J. E* **2001**, *4*, 411–417.
(28) Salis, A.; Pinna, M. C.; Bilaničová, D.; Monduzzi, M.; Lo Nostro, P.; Ninham, B. W. *J. Phys. Chem. B* **2006**, *110*, 2949–2956.
(29) Parsons, D. F.; Ninham, B. W. *Langmuir* **2010**, *26*, 1816–1823.
(30) Parsons, D. F.; Ninham, B. W. *J. Phys. Chem. A* **2009**, *113*, 1141–1150.
(31) Parsons, D. F.; Ninham, B. W. *Langmuir* **2010**, *26*, 6430–6436.
(32) Parsons, D. F.; Deniz, V.; Ninham, B. W. *Colloids Surf. A.* **2009**, *343*, 57–63.
(33) Parsons, D. F.; Ninham, B. W. *Colloids Surf. A* **2011**, *383*, 2–9.
(34) Jena, K. C.; Hore, D. K. *J. Phys. Chem. C* **2009**, *113*, 15364–15372.
(35) Pething, R. *Annu. Rev. Phys. Chem.* **1992**, *43*, 177–205.
(36) Richmoond, G. L. *Chem. Rev.* **2002**, *102*, 2693–2724.
(37) Zaia, D. A. M. *Amino Acids* **2004**, *27*, 113–118.
(38) McGuir, J. A.; Shen, Y. R. *Science* **2006**, *313*, 1945–1948.
(39) Dreesen, L.; Sartenaer, Y.; Humbert, C.; Mani, A. A.; Lemair, J. J.; Methivier, C.; Pradier, C. M.; Pradier, C. M.; Thiry, P. A.; Peremans, A. *Thin Solid Films* **2004**, *464−465*, 373–378.
(40) Boström, M.; Lima, E. R. A.; Tavares, F. W.; Ninham, B. W. *J. Chem. Phys.* **2008**, *128*, 135104(1)–135104(4).
(41) Kershner, R. J.; Bullard, J. W.; Cima, M. J. *Langmuir* **2004**, *20*, 4101–4108.
(42) Kosmulski, M. *Langmuir* **2002**, *18*, 785–787.
(43) Johnson, S. B.; Scales, P. J.; Healy, T. W. *Langmuir* **1999**, *15*, 2836–2843.
(44) Borah, J. M.; Das, M. R.; Mahiuddin, S. *J. Colloid Interface Sci.* **2007**, *316*, 260–267.
(45) Kunz, W. *Pure Appl. Chem.* **2006**, *78*, 1611–1617.
(46) Borah, J. M.; Sarma, J.; Mahiuddin, S. *Colloid Surf. A* **2011**, *375*, 42–49.
(47) Kunz, W.; Belloni, L.; Bernard, O.; Ninham, B. W. *J. Phys. Chem. B* **2004**, *108*, 2398–2404.
(48) Boström, M.; Williams, D. R. M.; Ninham, B. W. *Langmuir* **2001**, *17*, 4475–4478.
(49) Wernersson, E.; Kjellander, R. *J. Phys. Chem. B* **2007**, *111*, 14279–14284.
(50) Marcus, Y. *Pure Appl. Chem.* **1987**, *59*, 1093–1101.
(51) Boström, M.; Deniz, V.; Franks, G. V.; Ninham, B. W. *Adv. Colloid Interface Sci.* **2006**, *123−126*, 5–15.
(52) Su, C.; Suarez, D. L. *Clays Clay Miner.* **1997**, *45*, 814–825.
(53) Baltrusaitis, J.; Schuttlefield, J.; Jenson, J. H.; Grassian, V. H. *Phys. Chem. Chem. Phys.* **2007**, *9*, 4970–4980.
(54) Ponnurangam, S.; Chernyshova, I. V.; Somasundaran, P. *J. Phys. Chem. C* **2010**, *114*, 16517–16524.
(55) Wijnja, H.; Schulthess, C. P. *Soil Sci. Soc. Am. J.* **2000**, *64*, 898–908.
(56) Sprycha, R. J. *J. Colloid Interface Sci.* **1989**, *127*, 1–11.
(57) Grahame, D. C. *Chem. Rev.* **1947**, *41*, 441–501.
(58) Gierst, L.; Nicolas, E.; Tytgar-Vandenberghen, L. *Croat. Chem. Acta* **1970**, *42*, 117–141.
(59) Gierst, L.; Herman, P. Z. *Anal. Chem.* **1966**, *216*, 238–242.
(60) Sonnefeld, J.; Gobel, A.; Vogelsberger, W. *Polym. Sci.* **1995**, *273*, 926–931.
(61) Tschapek, M.; Wasowski, C.; Torres-Sanchez, R. M. *J. Electroanal. Chem.* **1976**, *74*, 167–176.
(62) Eagland, D.; Allen, A. P. *J. Colloid Interface Sci.* **1977**, *58*, 230–241.
(63) Heyda, J.; Lund, M.; Očán, M.; Slavíček, P.; Jungwirth, P. *J. Phys. Chem. B* **2010**, *114*, 10843–10852.
(64) Dumont, F.; Warlus, J.; Watillon, A. *J. Colloid Interface Sci.* **1990**, *138*, 543–554.
(65) Dumont, F.; Contreas, S.; Diazy Alonso, M. *An. Quim.* **1995**, *91*, 635–640.
(66) Dumont, F.; Verbeiren, P.; Buess-Herman, C. *Colloid Surf. A* **1999**, *154*, 149–156.
(67) Hidber, P. C.; Graule, T. J.; Gauckler, L. J. *J. Eur. Ceram. Soc.* **1997**, *17*, 239–249.
(68) Zhang, Y.; Cremer, P. S. *Proc. Natl. Acad. Sci. U. S. A.* **2009**, *106*, 15249–15252.
(69) Para, G.; Jarek, E.; Warszynski, P. *Adv. Colloid Interface Sci.* **2006**, *122*, 39–55.
(70) Lyklema, J. *J. Mol. Phys.* **2002**, *100*, 3177–3185.
(71) Lyklema, J. *Adv. Colloid Interface Sci.* **2003**, *100−102*, 1–12.
(72) López-León, T.; A. Jódar-Reyes, B.; Basto-González, D.; Ortega-Vinuesa, J. L. *J. Phys. Chem. B* **2003**, *107*, 5696–5708.
(73) Riés-Kautt, M. M.; Ducruix, A. F. *J. Biol. Chem.* **1989**, *264*, 745–748.
(74) Carbonnaux, C.; Riés-Kautt, M. M.; Ducruix, A. F. *Protein Sci.* **1995**, *5*, 2123–2128.
(75) López-León, T.; Elaïssari, A.; Ortega-Vinuesa, J. L.; Basto-González, D. *Chem. Phys. Chem.* **2007**, *8*, 148–156.
(76) López-León, T.; Santander-Ortega, M. J.; Ortega-Vinuesa, J. L.; Basto-González, D. *J. Phys. Chem. C* **2008**, *112*, 16060–16069.
(77) Vrbka, L.; Mucha, M.; Minofar, B.; Jungwirth, P.; Brown, E. C.; Tobias, D. J. *Curr. Opin. Colloid Interface Sci.* **2004**, *9*, 67–73.
(78) Bhatt, D.; Chee, R; Newman, J.; Radke, C. J. *Curr. Opin. Colloid Interface Sci.* **2004**, *9*, 145–148.
(79) Archntis, G.; Leontidis, E.; Andreou, G. *J. Phys. Chem. B* **2005**, *109*, 17957–17966.
(80) Pyper, N. C.; Pike, C. G.; Edwards, P. P. *Mol. Phys.* **1992**, *76*, 353–372.
(81) Craig, V. S. J.; Henry, C. L. In *Specific Ion Effect*; Kunz, W., Ed.; World Scientific: Singapore, 2010; Chapter 7 and references therein.
(82) Salis, A.; Bilaničová, D.; Ninham, B. W.; Monduzzi, M. *J. Phys. Chem. B* **2007**, *111*, 1149–1156.
(83) Robertson, T. B. *J. Biol. Chem.* **1911**, *9*, 303–326.
(84) Lyklema, J. *Chem. Phys. Lett.* **2009**, *467*, 217–222.
(85) Richardson, D. D. *J. Phys. A: Math. Gen.* **1975**, *8*, 1828–1841.
(86) Dagastine, R. R.; Prieve, D. C.; White, L. R. *J. Colloid Interface Sci.* **2000**, *231*, 351–358.
(87) Bergström, L.; Meurk, A.; Arwin, H.; Rowcliffe, D. J. *J. Am. Ceram. Soc.* **1996**, *79*, 339–348.
(88) Peterson, K. A.; Shepler, B. C.; Figgen, D.; Stoll, H. *J. Phys. Chem. A* **2006**, *110*, 13877–13883.